International Research Journal of Geology and Mining (IRJGM) (2276-6618) Vol. 3(4) pp. 147-157, May 2013
Available online http://www.interesjournals.org/IRJGM

Full Length Research Paper

The Bosumtwi meteorite impact crater, Ghana: New Results on the impact direction of the meteorite from 2D Electrical Resistivity Tomography (ERT) Survey

[1,2*]Akwasi Acheampong Aning, [1]Piotr Tucholka, [2]Sylvester K. Danuor

[1]Departement des Sciences de la Terre, Universitè Paris-Sud, Bat 504, F-91405 Orsay Cedex, France
[2]Department of Physics, Kwame Nkrumah University of Science and Technology, Kumasi, Ghana

Abstract

The 10.5 km diameter Bosumtwi meteorite impact crater in Ghana was formed about 1.07 million years ago. It is the source crater of the Ivory Coast tektites strewn field. The crater is occupied by a lake of diameter 8.5 km. Electrical resistivity tomography (ERT) survey using the multi-electrode gradient array was carried out along sixteen radial profiles around the lake to determine the sediment/bedrock contact, impact related structures and the impact direction of the meteorite. The data were corrected for topography and inverted using the L_1–norm. The subsurface images highlighted areas that are characterized by faults, fractures, lake sediments and impact related breccias such as allochthonous and parautochthonous breccias and dikes. The sediment/bedrock contact, which marks the crater geometry, was successfully mapped and it shows symmetry in the NE–SW direction and dips between 16^0 in the NE to 36^0 in the SW. The faults were mostly delineated in the west and they dip averagely 60^0 to the east and 80^0 to the west. The dips of the faults were statistically treated and were found to have a preferred direction. The results of the crater geometry and the orientation of the faults indicate that the meteorite came from the NE.

Keywords: Bosumtwi, Impact crater, electrical resistivity tomography, gradient array, inversion, faults, allochthonous, parautochthonous.

INTRODUCTION

Background information on the Bosumtwi impact crater

The Bosumtwi impact crater (Figure 1) is located about 30 km southeast of Kumasi in the Ashanti Region of Ghana. This complex terrestrial impact crater centered at $06^0 32'$N, $01^0 25'$W is the youngest (~1.07 Myr old) and best-preserved of about 95 terrestrial impact structures without modification of the crater morphology (Karp et al., 2002). It has a rim-to-rim diameter of about 10.5 km and is almost completely filled by Lake Bosumtwi which has a diameter of 8.5 km and a maximum depth of 75 m (Scholz et al., 2002). The crater is surrounded by a slight and irregular circular depression, as well as an outer ring of minor topographic highs.

The Ivory Coast tektite strewn field (Figure 1) which is associated with the Bosumtwi impact crater (Koeberl et al., 1997) was first reported in 1934 by Lacroix (1934), and three and a half decades later, more samples were recovered (Gentner, 1966; Saul, 1969). Microtektites were also found off the coast of West Africa (Glass, 1968; 1969) and are related to the tektites found on land.

Geophysical studies at the Bosumtwi crater area began in the 1960s when Jones et al. (1981) carried out gravity measurements around the lake and the results reflected only the regional trends. There is a negative Bouguer anomaly with amplitude of about –18 mgal and a diameter of about 13 km over the structure caused by the lower-density breccia, as is typical for impact structures (Grieve and Pilkington, 1996; Danuor, 2004). 3D gravity model by Ugalde et al. (2007) exhibits lateral density variations across the structure and also shows that the thickness of the intervals comprising polymict lithic impact breccia and suevite, monomict lithic breccia and fractured basement is much smaller than that predicted by numerical modeling.

*Corresponding Author Email:acheamponganing@gmail.com

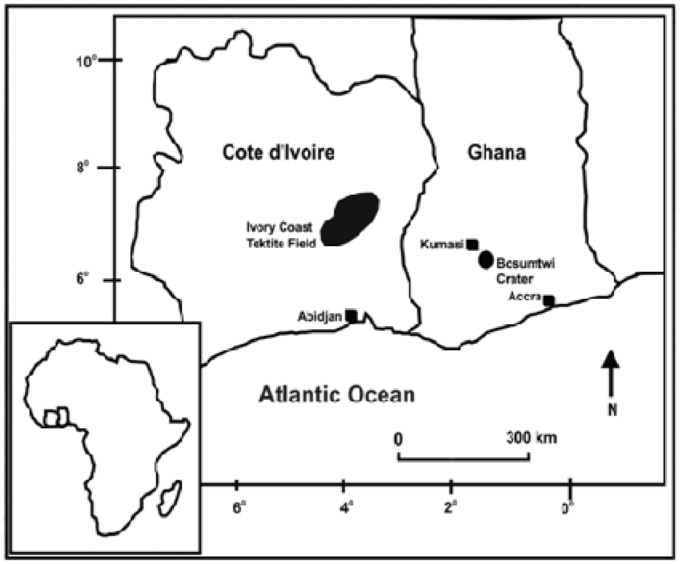

Figure 1. Overview of the Bosumtwi crater location and relation to the Ivory Coast tektite strewn field (Koeberl et al., 1998)

A high-resolution seismic survey was conducted in 1999 and 2000 and the results published by Karp et al. (2002) and Scholz et al. (2002). They found that the central uplift structure has a width of 1.8 km and a maximum height of 120 m above the top of the breccia. They reported that fracturing may be responsible for the relatively low velocity of 3.8 kms^{-1} in the crater floor. The post-impact sediments covering the crater structure are 180 – 300 m thick. The apparent crater depth, defined as the difference between the original target surface and the top of the breccia layer, is ~550 m, slightly deeper than several other complex impact structures on Earth of larger diameter. These show that the Bosumtwi impact structure is a small complex crater that deviates slightly from trends predicted from classical scaling laws (Grieve, 1991). Scholz et al. (2007), Schmitt et al. (2007) and Ugalde et al. (2007) detected that the central uplift has an overall irregular upper surface with a small graben structure. They also observed a series of normal faults that extend as much as 120 m into the sedimentary section above the central uplift and the decreasing density of fractures and micro cracks with depth.

Koeberl et al. (1997) and Pesonen et al. (1998; 1999; 2003) presented a more detailed information of the subsurface structure below and beyond the lake from a high-resolution aero geophysical survey data collected in 1997. Their findings include the possibility of a central uplift and delineation of two ring features, with one coinciding with the actual crater rim (ca. 11 km diameter), but they could not determine the origin of the outer ring feature (ca. 18 km diameter). Plado et al. (2000) and Elbra et al. (2007) reported that the normally magnetized remanence component in the suevites at the Bosumtwi crater area was acquired during the Jaramillo (starting at about 1.07 Myr) normal polarity epoch (Channell et al., 2002; Glass et al., 1991). Morris et al. (2007), Elbra et al. (2007), Coney et al. (2007), Deutsch et al. (2007), Morrow (2007) and Ugalde et al. (2007) did not find any evidence of the existence of the strongly magnetic impact-melt body underneath the lake sediments as reported by Jones et al. (1981), Artemieva et al. (2004) and Plado et al. (2000) after analyzing samples from the ICDP drill cores and modeling. Artemieva (2007) explained that the dispersion of impactites due to the vaporization of pore water, which was not included in the original numerical model, (Artemieva et al., 2004) is the most likely reason for the difference. In their model, they considered two types of targets: simple granite and a granite basement covered by 40 m thick sand layer but the target rocks at Bosumtwi comprise of meta greywackes and phyllites to slate. This is a major anomaly between the modelled results and the reality. These materials behave differently mechanically (Deutsch et al., 2007).

Though extensive work has been done on various scientific aspects of the Bosumtwi impact crater, no detailed mapping of the inner crater wall has been carried out to delineate the sediment/solid rock contact and therefore the exact crater geometry. The geometry of the crater, and the faults pattern and their preferred orientations has a direct link to the impact direction of the meteorite. Artemieva et al. (2004) found out from their numerical modeling that the impact direction was N-NE. In this paper we report on the use of the 2D electrical resistivity tomography (ERT) to map the inner crater geometry and the impact related structures including faults which have given new information on the impact direction of the Bosumtwi meteorite.

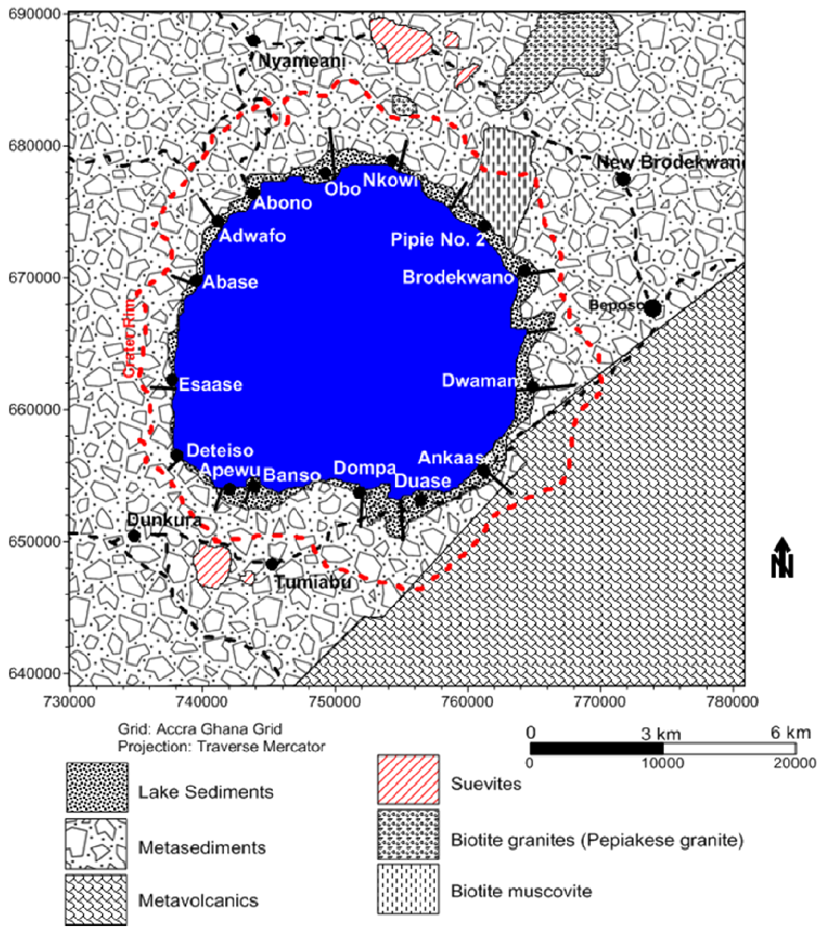

Figure 2. Geological map of the Bosumtwi crater area showing the profile lines that run radially along the lake shore (Modified from Koeberl and Reimold, 2005)

Geological setting

The Bosumtwi crater (Figure 2) was dug out in lower greenschist-facies supracrustal rocks of the 2.1 – 2.2 Gyr old Birimian Supergroup, comprising mainly metasediments and metavolcanics (Wright et al., 1985; Leube et al., 1990; Davis et al., 1994; Hirdes et al., 1996; Oberthür et al., 1998; Watkins et al., 1993; Koeberl and Reimold, 2005; Karikari et al., 2007; Coney et al., 2007).The Birimian target rocks are made up of mica schists and banded schists with both micaceous and quartz-feldspathic bands, phyllite, metagreywacke, quartzite and sandstone, shale and slate, as well as meta-tuffs. Birimian meta-volcanic rocks (altered basic intrusives intercalated with some metasediments) occur in the southeastern sector of the Bosumtwi area. Graywackes predominate the surface exposures and are the most important clast type in many suevite samples. Brecciated greywacke and phyllite dominate the geology immediately around the crater and locally intruded by small dikes and pods of granitic intrusives (Junner, 1937; Moon and Mason, 1967; Reimold et al., 1998; Koeberl and Reimold, 2005). Carbonate (calcite) which was previously unknown was identified in high abundance in the analysis of drill cores and their origin is pre–impact (Coney et al., 2007; Deutsch et al., 2007; Ferriére et al., 2007).

Other than the Obuom Range to the southeast of the crater, the topography of the Lake Bosumtwi drainage basin follows the Pleistocene relief produced by the impact structure. Lake morphometry is that of a simple bowl-shaped depression, which developed from the accumulation of post-impact lacustrine and alluvial sediments. The well-defined crater was initially characterized as a caldera (Smit, 1964) and has an average rim elevation of ~250 to ~300 m above the lake surface which is about 80–100 m below the terrain outside of the rim (Koeberl and Reimold, 2005). Except for the terrain of the Obuom mountain range, and locations along some stream channels in the environs of the crater, exposure is generally very poor.

Recent rock formations include the lake beds and the products of weathering (laterites, soil) which can have thicknesses up to 10 m. Although no impact melt rock has been found around the crater (Jones et al., 1981; Reimold et al., 1998), numerous breccia and suevite

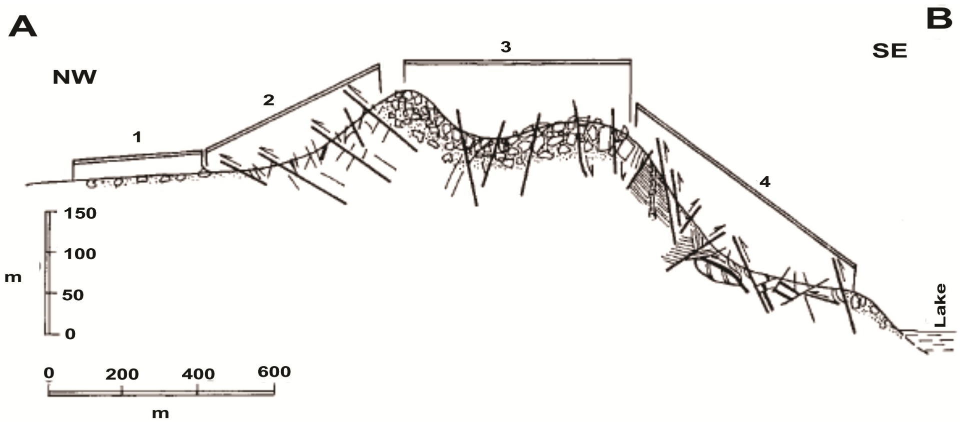

Figure 3. Zonation of the topography of NW part of the crater rim towards the lake (Reimold et al., 1998)

exposures have been mapped (Koeberl and Reimold, 2005). Recent drilling into the crater floor revealed that shales did indeed represent a major component of the target geology.

Meta-graywacke/phyllite rocks and granite from dikes seem to be important contributors to the compositions of the suevite and the road cut samples (fragmentary matrix), with a minor contribution of Pepiakese granite. The thickness of the fallout suevites outside the northern rim of the Bosumtwi crater is 15 m, and this facies occupies an area of about 1.5 km^2 (Boamah and Koeberl, 2002; 2003). The present distribution of the suevite is likely a result of differential erosion and does not reflect the initial distribution. Melt proportions are higher outside the crater rim, and this implies that much of the most heavily shocked material has been ejected from the crater. The relative amount of shocked and melted material in suevites from the central uplift is lower than in suevite from outside the northern crater rim (Coney et al., 2007; Ferriére et al., 2007).

Reimold et al. (1998) zoned a profile (Figure 3) in the northwestern part of the crater towards the lake into four after they carried out a structural analysis of the crater rim in NW-SE direction along the line A - B. Zone 4 is dominated by thrust faulting of multiple orientations, resulting in duplex-and lens-shaped bodies of pre-impact strata; zone 3 is made up of mega breccia with upward decreasing block sizes; zone 2consists of inward-dipping thrust planes, conjugate radial fractures, isoclinal folding, and overturned stratigraphy; and zone 1 is predominantly ejecta breccia cover and local mass wasting. The present study was conducted within zones 3 and 4. The above results (Figure 3) show that the inner crater (zone 4) is dominated by fractures and faults. One of the objectives of the research is to map the faults and determine their preferred orientation, which has a link to direction of the propagating shock waves.

MATERIALS AND METHODS

Electrical Resistivity Tomography (ERT) Survey

Resistivity imaging is becoming increasingly popular in electrical exploration, due to its ability to produce images of the subsurface efficiently and effectively as a result of the availability of automated data acquisition systems and efficient user friendly inversion software. It has been used to investigate areas of complex geology, such as volcanic and geothermal areas, seismotectonic structures, and areas of hydrogeologic phenomena and environmental problems, and the deposition and flow of impact melt and breccias (Steeples, 2001; Tong et al., 2010). With the development of innovative and robust inversion methods incorporating topography (Gunther et al., 2006; Loke and Barker, 1996), accurate data interpretation for resolving complex geological problems, such as defining aspects of hidden underground structures (i.e. fractures, water accumulations, etc.) or studying the spatiotemporal evolution of groundwater flow relative to landslide phenomena has become easier.

Though there have been electrical resistivity and magnetotelluric studies at impact crater sites, ERT has been hardly used in impact cratering studies (Kukkonen et al., 1992; Masero et al., 1997; Campos-Enriquez et al., 2004) despite the fact that it is becoming increasingly popular in electrical exploration, as a result of its ability to produce high resolution images of the subsurface. The only available data is the work by *The Geological Society of America* and the findings were published by Tong et al. (2010; 2012). They used ERT to study the deposition and flow of impact melt and breccias over the central uplift of the Araguainha impact structure in Brazil. They used the dipole-dipole array with eight electrodes (six current and two potential) and the electrode separation was 50 m.

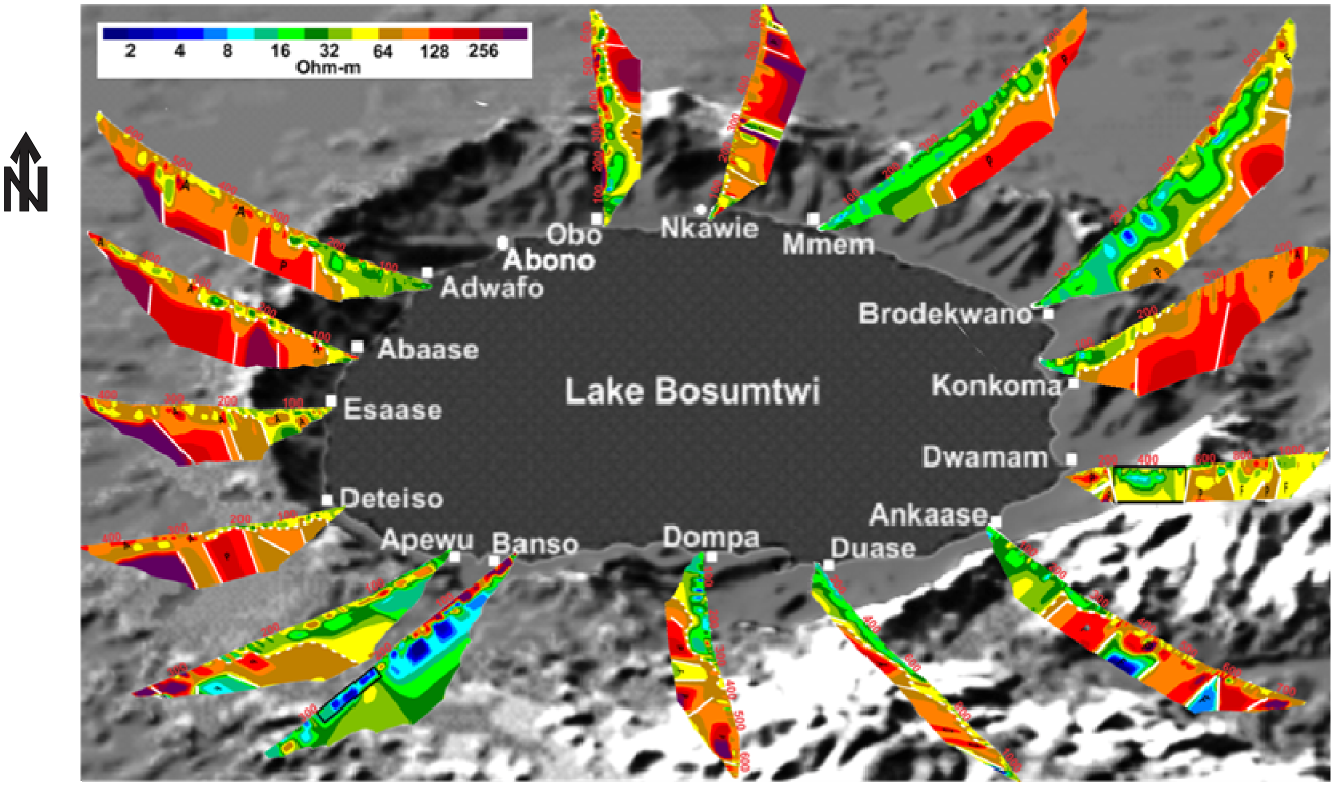

Figure 4. The Bosumtwi impact crater showing the 2D res of the various profiles and the communities located along the shore of the lake

METHODOLOGY

The multi-electrode ABEM Lund Imaging System (Dahlin, 1996) was used with the gradient array to acquire 16 electrical resistivity tomographs around the lake (Figure 4) starting from the shore and going uphill towards the rim of the crater. The survey profiles had a minimum electrode spacing of 5 m, and minimum and maximum lengths of 400 and 1,200 m respectively. The roll-along technique was used where the profile length was more than 400 m (Dahl and Schultz, 2001) to cover the entire length of the survey line where necessary.

The algorithm proposed by Loke and Barker (1996) for the automatic 2D inversion of apparent resistivity data was used. The data were topographically corrected and the L_1–norm (the robust) inversion technique was used in modeling the data. On electrical resistivity tomographies, fault zones can be easily delineated because they have lower resistivities than their surroundings as a result of their high permeability and high density of discontinuities. Faults are sometimes characterized by their sharp resistivities contrasts with their hosts. When the faults are filled with calcite or quartz they can have higher resistivity than their surroundings. Generally, faults occurring in crystalline environment are less resistive than the surrounding rock (Giocoli et al., 2008; Colella et al., 2004; Diaferia et al., 2006; Scheibz et al., 2009; Suzuki et al., 2000; Barsukov, 1970). The analysis of the resistivity images is based on the knowledge of the geology of the crater area and the topography on the profile. The fault lines were geostatistically treated using the von Mises and Fisher statistics.

RESULTS AND DISCUSSION

For uniformity in the interpretation of the different resistivity sections along various profiles, a common color code was adopted for presentation of the results (see Figure 4). The tomograms generally show a low surface resistivity towards the lake as expected due to the sediments, moderately high resistivity as one moves uphill towards the crater rim and high resistivity towards the end of the profile. The very low resistivity (< 64 Ω.m) (Figure 4) from the shore uphill towards the rim of the crater represents the post-impact lake sediments. The solid white lines are the inferred fault lines and the dotted white ones are the sediments and bedrock boundary. The blocks marked P and A are the interpreted parautochthonous and allochthonous breccias respectively and the low resistivity zones labeled F are fractures.

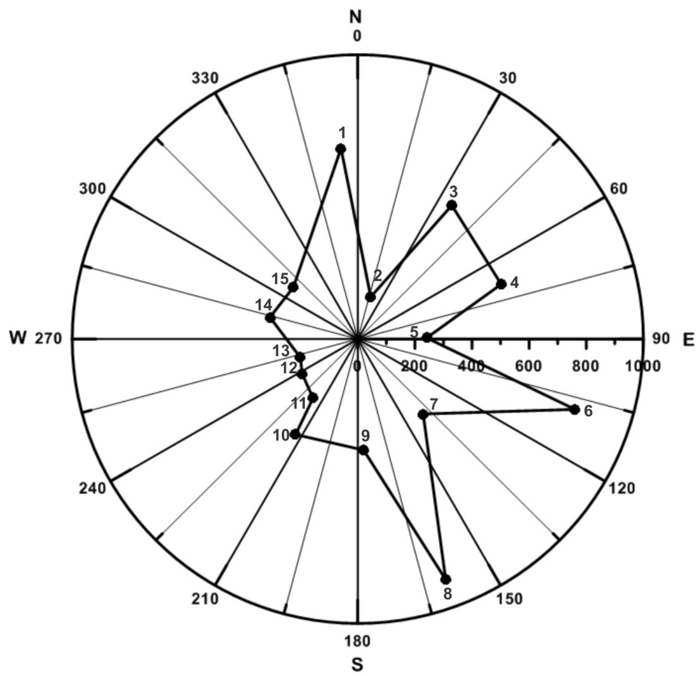

Figure 5. Radial plot of azimuth (location within the crater) relative to the center of the lake showing the extent of sediment distribution (solid line) within the inner crater; numbers 1 – 15 are the communities: 1– Obo; 2- Nkowie; 3- Mmem; 4- Brodekwano; 5- Konkoma; 6- Dwamam; 7- Ankaase; 8- Duase; 9- Dompa; 10- Banso; 11- Apewu; 12- Detieso; 13- Esaase; 14- Abaase and 15- Adwafo

The post-impact lake sediments and the talus

For all the profiles the results show a region of low resistivity (< 64 Ω.m) from the shore of the lake towards the crater rim (Figure 4). These low resistivity zones have been interpreted as the lake sediments. The zones thin out as one move uphill towards the rim. The extent of the sediments around the lake is asymmetrical (Figure 4) with the eastern and southern portions of the lake having the largest and deepest extents whilst the western portion has the shortest and thinnest.

To have a better view of the limit of the sediments around the lake, an azimuthal plot showing the extent of the sediments in the various communities (numbered 1 – 15) was generated as shown in Figure 5. In the plot, the 8.5 km lake is assumed to be a point located at the center, and the sediments extend from the shore of the lake towards the crater rim. The solid line marked the extent of the sediments (Figure 5), and therefore the sediments/solid rock contact.

A considerable amount of talus was observed around the lake. The amount increases as one moves downhill towards the lake. It is abundant on the western portion of the crater with Abaase (No. 14) having the highest quantity of talus material. Even though a small quantity of talus was observed in the Obo (No. 1) area, the profile there shows very high near surface resistivities.

The bedrock

The areas with resistivity > 64 Ω.m were labelled as the bedrock which consists of metagray wackes, phyllites and slates. With the exception of Dwamam and Banso all the others evidently show the sediments and target surface boundary. The dipping of the bedrock is the same as that of the sediments (Figures 4 and 5). The target appears to have been severely faulted and downthrown between 200 and 500 m on the Dwamam resistivity image. The Banso tomogram is within the post impact sediments. The target ground has been brecciated and faulted all around the crater, but the degree of fracturing is less on the western part of the crater.

Bilateral symmetry discovery is very essential in restricting the direction of an oblique impact (Poelchau and Kenkman, 2008).The gradient of the bedrock surface shows a bilaterally symmetric pattern (Figure 6) with the symmetry axis running NE–SW. The north which is symmetrical to the east has comparable dip values of 19^0 and 17^0 respectively; the NW and the SE have 19^0 and

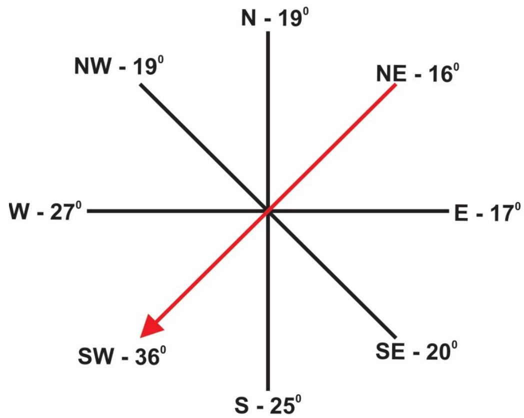

Figure 6. Radial plot of azimuth (location within the crater) relative to the center of the lake showing the gradient of the sediment/bedrock contact dipping NE-SW

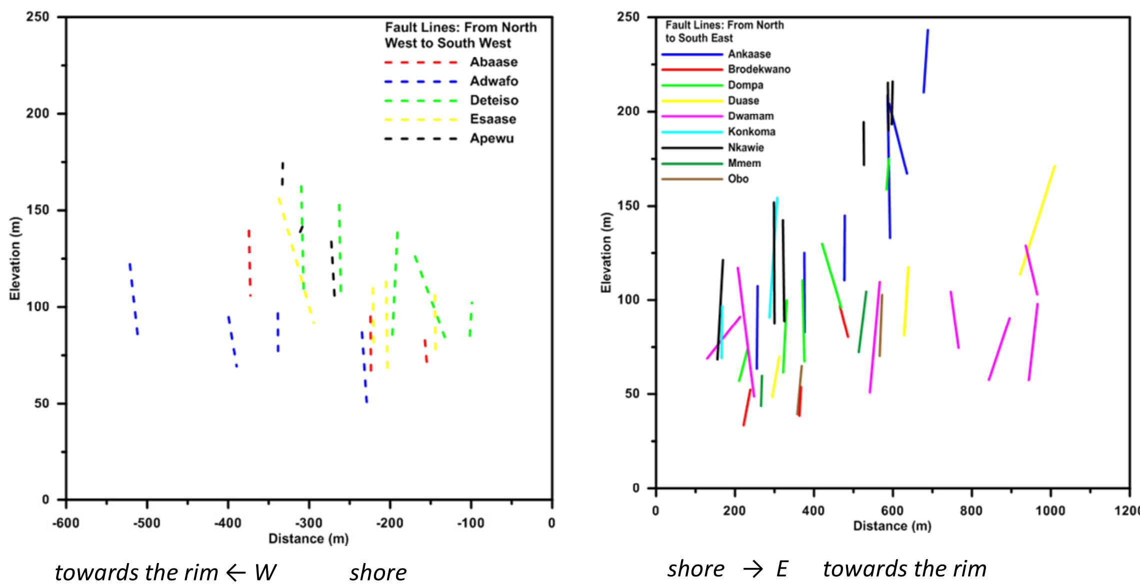

(a) (b)

Figure 7. Dips of the inferred faults around the lake: (a) Western section and (b) Eastern section; for the two figures the zero on the x-axis is the shore of the lake

20^0 and finally the west and south have 27^0 and 25^0 respectively.

In general, the sediment/bedrock surface dips between 16^0 in the NE to 36^0 in the SW as shown in Figure 6.

The faults and fractures

With the exception of the Banso traverse which was within the sediments, faults were identified on all the profiles (Figure 4). Generally, the faults on the western side of the crater dip more steeply (nearly vertical) than those on the east (Figures 7a and 7b). Reverse faults (faults dipping away from the center of the crater) were mapped in the northeast; southeast and southwest (see Figure 4). Reflecting the results displayed in Figure 7a, there is a fault line at around 240 m on the Adwafo, Abaase and Esaase profiles (see Figure 4). This could be the same fault line forming a semi-concentric fault on the west and northwest part of the crater. There are other similarities as well: e.g. 200 and 300 m on Esaase and Deteiso and 270 m on Deteiso and Apewu traverses. These faults could all be related.

There is no noticeable link between the faults on the eastern section of the crater. Fracture zones (areas with resistivities < 64 Ω.m that are far from the shore and not

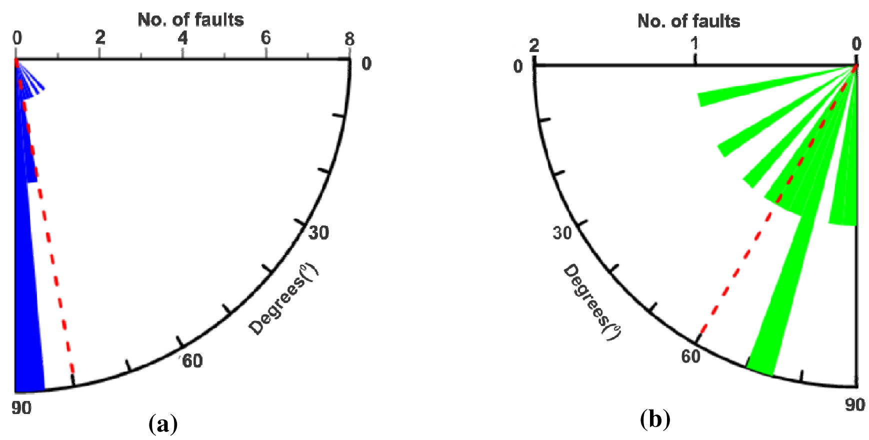

Figure 8. Rose plots of the inferred faults on the west section (a), and east section (b) of the lake indicating the angles of dip. The dotted line is the mean dip of the fault lines

Table 1. Mean directions and standard errors of the fault lines

Section of the crater	N	θ_m	R	R_m	R_c	κ	S_e
East	10	60.33	9.32	0.93	0.54	7.73	6.85
West	16	79.62	15.67	0.98	0.43	25.25	2.88

n: number of samples; θ_m: mean direction; R: resultant length; R_m: mean resultant length;
R_c: Rayleigh's test for critical values of R_c at 5% level of significance; κ: concentration parameter;
s_e: standard error

on the surface of the tomograms) were mapped on all the traverses on the southeastern portion of the crater (Figure 4). They were interpreted as open fractures filled with polymict breccias in a heterogeneous matrix. The dips of the faults and/or fractures average about $60^0$and $80^0$for the east and west sections of the crater respectively and this is consistent with the findings of Reimold et al. (1998) and Hunze and Wonik (2007). Hunze and Wonik (2007) on their analysis of the televiewer images from the central uplift borehole LB–08A, found that most of the fractures were towards the SE. Could this have a relation with the numerous fractures found on the SE profiles (especially Dwamam and Ankaase)? It is however know that the topography outside the Bosumtwi crater rim is nearly horizontal (Koeberl and Reimold, 2005), therefore the increase in dip angles towards the southwest part is as a result of it being in the downrange direction of the oblique impactor.

Statistical analysis of the faults

The von Mises distribution and Fisher statistics were used to characterize the dip of the faults identified on the eastern and western parts of the crater (Figure 8 and Table1). The resultant length, *R*, the mean resultant length, R_m, the mean direction, θ_m and the standard error, s_e, were calculated and the values of the concentration parameter, κ, estimated using the maximum likelihood estimates of the concentration parameter from calculated values of R_m adapted from Batschelet (1965), and Gumbel, Greenwood, and Durand (1953). The measure of dispersion (test for randomness) values R_m and κ exhibit high values in the west.This indicates that the directional measurements in this section are very close to the mean direction (see Figure 8 and Table 1).

The Rayleigh's test for critical values of R_c at 5% level of significance was also estimated (Table 1) using statistical table for the critical values of *R* for the presence of a preferred trend with level of significance α from the number of samples *n* adapted from Mardia (1972). The critical values were smaller than the computed values (R_m) and the hypothesis is that, the geologic feature (faults) was not uniformly circularly distributed and the null hypothesis which states that κ =0 for circularly distributed data could not be accepted; therefore the faults have a preferred direction.

In trying to find the preferred direction of the faults, the crater has been divided into west and east with respect to the center of the lake. The rose diagrams (Figure 8) show how the faults have been bunched together. This demonstrates that they have a preferred direction and

Table 2. Resultants of the sampled and pooled fault lines

Section of the crater	N	R_T	R_p	R_{ps}	κ	F_T	F_c
East-West	26	24.98	24.68	0.95	10.27	7.78	4.26

N: number of pooled samples; R_T: the sum of the resultants of the faults in the east and west portions of the lake; R_p: resultant length of pooled faults; R_{ps}: standardized resultant of pooled faults; κ: concentration parameter; F_T: test value and F_c critical value 5% level of significance

are not randomly distributed. As shown in Figure 4, the faults dip steeply towards the lake center. In Table 1, the standard error, s_e, indicates the limits of the precision of θ_m, the mean direction.

From the results, it is clear that the faults on the west section have their preferred direction close to the mean direction (dotted line).

The Fisher statistics was used for the comparison of the two mean directions (East and West). The resultant length R_p, the standardized resultant R_{ps} of the pooled vectors, the test values, F_T, and the number of pooled vectors, N, were calculated and the critical values F_c at 5% were estimated from Fisher statistical tables with two degrees of freedom, 1 and 24. From Table 2, the observed statistics of the test value F_T exceeds the tabulated F_c value at the 5% level of significance; this indicates that the two mean directions are different meaning that they are not from the same population.

The interpretation of the fault lines in the crater indicates that the impactor came from the NE as greater proportion of the energy (momentum) was in the downrange (SW) direction and this portion of the crater experienced a greater degree of faulting. This preferential direction of faulting shows the transport direction of the material and indicates the impact vector. The analysis of the slopes of the bedrock also supports a NE impactor.

Summarizing the results, it is noted that the bilateral symmetry exhibited by the bedrock surface is an indication for the restriction of the direction of an oblique impactor. It has been established that the increase in dip angles towards the southwest part is as a result of that section being in the downrange direction of the oblique impactor.

CONCLUSION

Electrical resistivity tomography (ERT) has been used successfully at the Bosumtwi impact crater to map the inner wall of the crater, delineate the sediment and bedrock contact and other impact related structures of this topographically varied environment. From the results, it is inferred that the area extending from the lake shore towards the crater rim contains essentially three formations. First, the low resistivity regions < 64 Ω.m represent the lake sediments. Second, the moderately high resistivity regions with values between 128 and 200 Ω.m have been interpreted as impact related breccias or allochthonous materials. Third, the high resistivity regions > 128 Ω.m at the base of the tomograms represent the basement metamorphic rocks which are made up of metavolcanic and metasedimentary rocks. The ERTs also highlighted areas characterized by faults and dikes.

The sediment/bedrock contact dips between the lowest of 16° in the NE to the highest of 36° in the SW. The sediment/bedrock surface is symmetrical in the NE–SW direction. Evidence of bilateral symmetry as exhibited by the gradient of the bedrock surface supports strongly an oblique impact. Also, the increase in dip angles towards the southwest is as a result of that section being in the downrange part of the oblique impactor.

Statistical analysis of the faults revealed that the mean directions of the faults in the east and the west are different and that they are not randomly distributed but have a preferred direction. However, the individual directional measurements of the faults in the west are closer to their mean direction than those in the east. Therefore, the faults in the west, and consequently those in the SW have their origin most likely as a result of the impact. The findings therefore point to the fact that the meteorite most probably came from the NE.

ACKNOWLEDGEMENTS

The research was funded by Kwame Nkrumah University of Science and Technology (KNUST), Kumasi, and Laboratoire IDES-UMR 8148, Université Paris Sud and the French Embassy, Ghana. We wish to thank the Bosumtwi District Assembly, Ghana for granting our research. We also thank the students and service personnels at KNUST, and all the people in the communities around Lake Bosumtwi who helped us to acquire the data.

REFERENCES

Artemieva N (2007). Possible reasons of shock melt deficiency in the Bosumtwi drill cores. *Meteoritics and Planetary Science 42*(4/5):883–894.

Artemieva N, Karp T, Milkereit B (2004). Investigating the Lake Bosumtwi impact structure: Insight from numerical modeling.

Geochem. Geophys. Geosys.: An Electr. J. Earth Sci.; 5:11.
Barsukov OM (1970). Relationship between the electrical resistivity of rocks and tectonic processes,Izv.Acad. Sci., USSR Phys. Solid Earth, Engl. Transl. (1):55–59.
Boamah D, Koeberl C (2002). Geochemistry of soils from the Bosumtwi Impact Structure, Ghana, and relationship to radiometric airborne geophysical data. – In: J. PLADO and L. PESONEN (Eds.): Meteorite Impacts in Precambrian Shields. *Heidelberg – Berlin (Springer) Impact Studies;* 2: 211–255.
Boamah D, Koeberl C (2003). Geology and geochemistry of shallow drill cores from the Bosumtwi Impact Structure, Ghana.*Meteoritics and Planetary Science* 38:1137–1159.
Campos-Enriquez JO,. Chavez-Garcia FJ, Acosta-Chang JG, Marsui T, Arzate JA, Unsworth MJ, Ramos-Lopez J (2004). Shallow crustal structure of Chicxulub impact crater imaged with seismic, gravity and magnetotelluric data: Inferences about the central uplift. Geophys. J. Int.; 157:515–525.
Channell J, Mazaud A, Sullivan P, Turner S, Raymo M (2002). Geomagnetic excursions and paleointensities in the 0.9–2.15 Ma interval of the MatuyamaChron at ODP Site 983 and 984 (Iceland basin).J. Geophys. Res.; 107/6:1–14, doi: 10.1029/2001JB000491.
Colella A, Lapenna V, Rizzo E (2004). High-resolution imaging of the high Agri valley basin (Southern Italy) with the electrical resistivity tomography.*Tectonophysics 386*(1-2), 29–40.
Coney, L., R. L. Gibson, W. U. Reimold, and C. Koeberl (2007).Lithostratigraphic and petrographic analysis of ICDP drill core LB-07A, Bosumtwi Impact Structure, Ghana.*Meteoritic and Planetary Science* 42(4/5):569–589.
Dahl JM, Schultz PH (2001).Measurement of stress wave asymmetries in hypervelocity projectile impact experiments. Int. J. Impact Engine.; 26:145–155.
Dahlin T (1996).2D resistivity surveying for environmental and engineering applications. *First Break* 14:275–284.
Danuor SK (2004). Geophysical investigations of the Bosumtwi Impact Crater and comparison with terrestrial meteorite craters of similar age and size.Ph.D.thesis, Kwame Nkrumah University of Science and Technology, Kumasi, Ghana.
Davis DW, Hirdes W, Schaltegger U, Nunoo EA (1994). UPb age constraints on deposition and provenance of Birimian and gold-bearing Tarkwaian sediments in Ghana, West Africa. Precambrian Res.; 67:89–107.
Deutsch A, Luetke S, Heinrich V (2007). The ICDP Lake Bosumtwi impact crater scientific drilling project (Ghana): Core LB-08A litho-log, related ejecta, and shock recovery experiments. *Meteoritics and Planetary Science* 42(4/5):635–654.
Diaferia I, Barchi M, Loddo M, Schiavone D, Siniscalchi A (2006). Detailed imaging of tectonic structures by multiscale earth resistivity tomographies: The Colfiorito normal faults (Central Italy):.Geophys. Res. Letters; 33(9):L09305.1–L09305.4.
Elbra T, Kontny A, Pesonen LJ, Schleifer N, Schell C (2007). Petrophysical and paleomagnetic data of drill cores from the Bosumtwi Impact Structure, Ghana. *Meteoritics and Planetary Science* 42(4/5):829–838.
Ferriére L, Koeberl C, Reimold UW, Mader D (2007). Drill core LB-08A, Bosumtwi Impact Structure, Ghana: Geochemistry of fallback breccia and basement samples from the central uplift. *Meteoritics and Planetary Science 42*(4/5):689–708.
Ferriére L, Koeberl C, Reimold UW (2007). Drill core LB-08A, Bosumtwi impact structure, Ghana: Petrographic and shock metamorphic studies of material from the central uplift. *Meteoritic and Planetary Science* 42(4/5):611–633.
Gentner W (1966).Auf der SuchenachKratergläsern, Tektiten und Meteoriten in Afrika. *Naturwissenschaften* 12:285–289.
Giocoli A, Magri C, Vannoli P, Piscitelli S, Rizzo E, Siniscalchi S, Burrato P, Basso C, Nocera CD (2008). Electrical resistivity tomography investigations in the Ufita Valley (Southern Italy).*Annals of Geophysics* 51(1):213–223.
Glass BP (1968). Glassy objects (microtektites?) from deep sea sediments near the Ivory Coast. *Science* 161:891–893.
Glass BP, Kent DV, Schneider DA, Tauxe L (1991). Ivory Coast microtektite strewn field: Description and relation to the Jaramillo geomagnetic event. *Earth and Planetary Science Letters 107*, 182–196.
Glass BP (1969). Chemical composition of Ivory Coast microtektites.*GeochimicaetCosmochimicaActa 33*:1135–1147.
Grieve RAF, Pilkington M (1996). The geophysical signature of terrestrial impacts.*AGSO* J. Austr. Geol. Geophys.; 16:399–420.
Grieve, R. A. F. (1991). Terrestrial impact: The record in the rocks. *Meteoritics* 26:175–194.
Gunther T, Rucker C, Spitzer K (2006). Three dimensional modeling and inversion of dc resistivity data incorporating topography–II Inversion. Geophys. J. Int.; 166:506–517.
Hirdes W, Davis DW, Ludtke G, Konan G (1996). Two generations of Birimian (Paleoproterozoic) volcanic belts in northeastern Cote d'Ivoire (West Africa): Consequences for the–Birimian controversy. Precambrian Res.; 80:173–191.
Hunze S,. Wonik T (2007). Lithological and structural characteristics of the Lake Bosumtwi Impact Crater, Ghana: Interpretation of acoustic televiewer images. *Meteoritics and Planetary Science* 42(4/5):779–792.
Jahrbuch der GeologischenBundesanstalt (Vienna, Austria) (Yearbook of the Geological Survey of Austria) 143:581–604.
Jones WB, Bacon M, Hastings DA (1981). The Lake Bosumtwi Impact Crater, Ghana. *Geological Society of America Bulletin;* 92:342–349.
Junner NR (1937). The geology of the Bosumtwi caldera and surrounding country. *Gold Coast Geological Survey Bulletin;* 8:1–38.
Karikari F, Ferriére L, Koeberl C, Reimold WU, Mader D (2007). Petrography, geochemistry, and alteration of country rocks from the Bosumtwi Impact Structure, Ghana.*Meteoritics and Planetary Science* 42(4/5):513–540.
Karp T, Milkereit B, Janle P, Danuor SK, Pohl P, Berckhemer H, Scholz CA (2002). Seismic investigation of the Lake Bosumtwi impact crater: Preliminary results. *Planetary and Space Science* 50:735–743.
Koeberl C, Bottomley RJ, Glass BP, Storzer D (1997).Geochemistry and age of Ivory Coast tektites and microtektites.*Geochimicaet CosmochimicaActa* 61:1745–1772.
Koeberl C, Reimold WU (2005, June). Bosumtwi Impact Crater, Ghana (West Africa): An Updated and Revised Geological Map, with Explanations. *Jahrbuch der Geologischen Bundesanstalt* 145(1): 31–70.
Koeberl C, Reimold WU, Blum JD, Chamberlain CP (1998).Petrology and geochemistry of target rocks from the Bosumtwi Impact Structure, Ghana, and comparison with Ivory Coast tektites.*Geochimicaet CosmochimicaActa* 62:2179– 2196.
Koeberl C, Reimold WU, Pesonen LJ, Brandt D (1997). New studies of Bosumtwi Impact Structure, Ghana: The 1997 field season. *Meteoritic and Planetary Science 32*, A72–A73 (Abstract).
Kukkonen IT, Kivekas L, Paananen M (1992).Physical properties of karnaite (impact melt), suevite and impact breccia in the Lappajarvimetorite crater, Finland.*Tectonophysics* 216:111–122.
Lacroix A (1934). Sur la découverte de tectites à la Côte d'Ivoire. *Comptes Rendus Academie des Sciences Paris* 199:1539–1542.
Leube A, Hirdes W, Mauer R, Kesse GO (1990).The early Proterozoic BirimianSupergroup of Ghana and some aspects of its associated gold mineralization. Precambrian Res.; 46:139–165.
Loke MH, Barker RD (1996). Rapid least-squares inversion of apparent resistivity pseudosections by a quasi-Newton method. *Geophysical Prospecting* 44:131–152.
Masero W, Fischer G, Schnegg PA (1997). Electrical conductivity and crustal deformation from magnetotelluric results in the region of the Araguainha impact, Brazil. Physics of the Earth and Planetary Interiors 101:271–289.
Moon PA, Mason D (1967). The geology of 1/4^{o} field sheets 129 and 131, Bompata S.W and N.W. Ghana Geological Survey Bulletin 31:1–51.
Morris WA, Ugalde H, Clark C (2007). Physical property measurements: ICDP boreholes LB-07A and LB-08A, Lake Bosumtwi Impact Structure, Ghana. *Meteoritics and Planetary Science 42*(4/5):801–809.
Morrow JR (2007). Shock-metamorphic petrography and microRaman spectroscopy of quartz in upper impactite interval, ICDP drill core LB-07A, Bosumtwi Impact Crater, Ghana. *Meteoritic and Planetary Science 42*(4/5):591–609.
Oberthür T, Vetter U, Davis DW, Amanor JA (1998). Age constraints on

gold mineralization and palaeoproterozoic crustal evolution in the Ashanti belt of southern Ghana. *Precambrian Research 89*:129–143.

Pesonen LJ, Koeberl C, Hautaniemi H (2003). Airborne geophysical survey of the Lake Bosumtwi meteorite impact structure (Southern Ghana) – Geophysical maps with descriptions.

Pesonen LJ, Koeberl C, Ojamo H, Hautaniemi H, Elo S, Plado P (1998). Aerogeophysical studies of the Bosumtwi Impact Structure, Ghana (abstract). *Geological Society of America Abstract with Programs* 30(7):A–190.

Pesonen LJ, Plado J, Koeberl C, Elo S (1999). The Lake Bosumtwi meteorite impact structure, G: Magnetic modelling (abstract). *Meteoritics and Planetary Science* 34:A91–A92.

Plado J, Pesonen LJ, Koeberl C, Elo S (2000). The Bosumtwi meteorite impact structure, Ghana: A magnetic model. *Meteoritic and Planetary Science 35*, 723–732.

Poelchau MH, Kenkman T (2008). Asymmetric signatures in simple craters as an indicator for an oblique impact direction.*Meteoritics and Planetary Science* 43:2059–2072.

Reimold WU, Brandt D, Koeberl C (1998, June). Detailed structural analysis of the rim of a large, complex impact crater: Bosumtwi Crater, Ghana. *Geology* 26(6):543–546.

Saul JM (1969). Field investigations at Lake Bosumtwi (Ghana) and in the Ivory Coast tektite strewn field Natl. Geograph. Soc. Res. Reports; 1964 Proj: 201–212.

Scheibz J, Haeusler H, Kardeis G, Kohlbeck F, Chwatal W, Figdor H, Koenig C (2009). Geologic interpretation of geophysical investigations in the Oslip section, Rust Range, Northern Burgenland, Austria, in European Geosciences Union: Vienna, Austria. Geophysical Research Abstracts 11:10559.

Schmitt DR, Milkereit B, Karp T, Scholz CA, Danuor SK, Meillieux D, Welz M (2007). In situ seismic measurements in borehole LB-08A in the Bosumtwi Impact Structure, Ghana: Preliminary interpretation. Meteoritics and Planetary Science 42(4/5):755–768.

Scholz CA, Karp T, Brooks TM, Milkereit M, Amoako PYO, Arko JA (2002). Pronounced central uplift identified in the Bosumtwi Impact Structure, Ghana, using multichannel seismic reflection data. Geology 30:939–942.

Scholz CA, Karp T, Lyons RP (2007). Structure and morphology of the Bosumtwi impact structure from seismic reflection data. Meteoritic and Planetary Science 42(4/5):549–560.

Smit AFJ (1964). Origin of Lake Bosumtwi (Ghana).Nature 203:179–180.

Steeples DW (2001). Engineering and environmental geophysics at the millennium.Geophysics 66, 31–35.

Suzuki K, Toda S, Kusunoki K, Fujimitsu Y, Mogi T, Jomori A (2000). Case studies of electrical and electromagnetic methods applied to mapping active faults beneath the thick Quaternary. Engineering Geology 56(1-2):29–45.

Tong CH, Elis VR, Lana C, Marangoni YR (2012, 03 February). Electrical Imaging of Impact Structures.

Tong CH, Lana C, Marangoni YR, Elis VR (2010).Geoelectric evidence for centripetal resurge of impact melt and breccias over central uplift of Araguainha impact structure. Geology 38:91–94.

Ugalde H, Danuor SK, Milkereit B (2007).Integrated 3-D model from gravity and petrophysical data at the Bosumtwi Impact Structure, Ghana.Meteoritics and Planetary Science 42(4/5):859–866.

Ugalde H, Morris WA, Pesonen LJ, Danuor SK (2007). The Lake Bosumtwi meteorite impact structure, Ghana– Where is the magnetic source? Meteoritics and Planetary Science 42(4/5):867–882.

Watkins AP, Iliffe EJ, Sharp WE (1993). The effects of extensional and transpressional tectonics upon the development of the Birimian sedimentary facies in Ghana, W. Africa: Evidence from the Bomfa/Beposo District, near Konongo. J. Afri. Earth Sci.; 17:457–478.

Wright JB, Hastings DA, Jones WB, Williams HR (1985). Geology and Mineral Resources of West Africa. Geology and Mineral Resources of West Africa. Allen and Unwin.